EFFECTS OF SKI STIFFNESS IN A SEQUENCE OF SKI TURNS

M. MÖSSNER[1], D. HEINRICH[1], P. KAPS[2], H. SCHRETTER[3], and W. NACHBAUER[1]

[1] Department of Sport Science, University of Innsbruck, Austria

[2] Department of Engineering Mathematics, University of Innsbruck, Austria

[3] HTM Tyrolia, Schwechat, Austria

KEY WORDS: Alpine skiing, simulation, ski turns, ski-snow interaction, ski stiffness

INTRODUCTION

Material properties like ski stiffness can be evaluated by field experiments or simulation calculations. Field measurements benefit from closeness to reality but often are difficult to reproduce. In every new run there always will be some, perhaps negligible, changes. Therefore, it is hard to judge whether observed effects are due the varied ski stiffness or something else. On the other hand in simulation it is quite simple to study the influence of a single parameter by redoing the calculations with varied stiffness data. It is not necessary to build ski prototypes. Further, investigated stiffness variations can be rather large. Although simulation lacks from incomplete modeling it is a valuable tool in investigating the effect of a single or a few parameters.

In so called carved turns the ski tries to follow the circle given by the bended ski edge. Such turns cause little energy loss due to shearing. Only highly skilled skiers are able to achieve purely carved turns. The nowadays widely used carving skis notably support the carving technique. But, except for very hard snow conditions, skis always skid to some extent. As outlined in this paper, ski stiffness has an important impact on the amount of skidding. Proper modeling of the ski-snow interaction is essential for simulation of skiing. In several published studies elastic snow penetration laws are used (Lieu and Mote [9], Renshaw and Mote [19], Tada and Hirano [21], Kaps et al. [8], Casolo et al. [2], Nordt et al. [18], or Bruck et al. [1]). Elastic snow penetration forces produce a too small penetration depth for the rear part of the ski and consequently too small side forces. A hypoplastic force-penetration relation as suggested by Mössner et al. [14] or Federolf [3] overcomes these problems since it causes almost the same penetration depth from the bindings

to the end of the ski. In our work we started by modeling a sledge on two skis carving a single turn with constant edge angle [14], then the model was improved to perform a sequence of turns [15], and recently the sledge was replaced by a Hanavan type model of the skier [6]. A hypoplastic constitutive equation was used for the penetration force and orthogonal metal cutting theory for the shearing force of the snow. The simulation model was validated in the case of a single turn with constant edge angle. First parameter studies were presented by Heinrich et al. [5] and Mössner et al. [16]. In this study we used the model of [15] to investigate the influence of ski stiffness on the trajectory of the skier performing a sequence of turns.

METHOD

Model of the Skier-Ski System

Skier, skis, and bindings (Fig. 1) were assembled in the multibody system software LMS Virtual.Lab [12]. The skier was modeled as one rigid body with given mass and moment of inertia. It was connected by rotational joints with two weightless shanks with ski boot soles. Each boot sole was connected to the bindings by spherical joints. The binding-ski connections were a bracket joint for the toe piece and a translational joint for the heel piece. Each ski consisted of 18 rigid segments and a shovel segment. The segments were linked by revolute joints that allowed rotation around the transversal (bending) and the longitudinal (torsion) axes. The spring and damping constants for the springs in these joints were adapted to experiments on real skis. The position of the skier's center of mass was fixed. For the rotational joints between the skier and the shanks driving constraints were implemented to steer the edge angles of the two skis during the simulation.

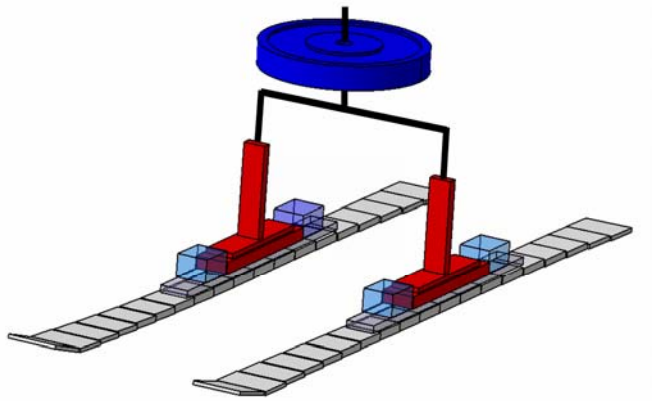

Fig. 1: The skier-ski system in the LMS Virtual Lab software.

Forces Applied to the Skier-Ski System

Since the skis were modeled by rigid cuboids, the bottom surface of each ski was not smooth and the edge was even discontinuous. Therefore, we attached a differentiable surface to the bottoms of the ski segments, which is called running

surface of the ski. Each point of the bottom rectangles of the multibody system model uniquely corresponds to one point of the running surface. Forces were calculated with respect to this surface and were supplied to the multibody system model via the corresponding point of the cuboid-shaped ski segment. For ski-snow contact forces, three types of forces were considered: 1) the penetration force normal to the snow surface, 2) the shear force transversal to the ski edge, and 3) the friction force in tangential direction.

The reaction force normal to the snow surface was modeled by a hypoplastic force-penetration relation (see Fellin [4]). For the force calculations each segment was divided into 16 sub-segments. Further, the sub-segments were assumed to follow the bending and the torsion of the running surface. For the description of a point of the running surface of the ski we introduced the coordinates ξ and η for the longitudinal and the transversal directions of the ski, respectively. ξ starts from zero at the end to L_S at the tip of the ski and η ranges from $-w$ to $+w$ from the right to the left ski edge. Let L be the length of a sub-segment, θ the edge angle, $\varepsilon=e(\xi,\pm w)$ the penetration depth of the ski edge orthogonal to the snow surface. Then one gets for the volume of displaced snow

$$V = \frac{L\,\varepsilon^2}{2\tan\theta}. \tag{1}$$

For the hypoplastic force-penetration relation one has to distinguish between loading and unloading of snow. For this we computed the maximum penetration depth of all frontal sub-segments of the ski

$$e_{\max}(\xi,\eta) = \max_{s>\xi} e(s,\eta). \tag{2}$$

Let ε_{max} be the value of $e_{\max}$ for the ski edge. Further, let H be the snow hardness (Mössner et al. [13,17]). Then one gets for the snow penetration force

$$F_p = \begin{cases} H\,V, & \varepsilon = \varepsilon_{\max} \quad (loading) \\ H\,V\,f(\varepsilon/\varepsilon_{\max}), & \varepsilon < \varepsilon_{\max} \quad (unloading) \end{cases}. \tag{3}$$

Since compacted snow shows hardly any elastic response the scaling function f drops very fast from 1 to 0. Setting $f_1=0.8$ and $f_2=0.9$ we use

$$f(s) = \begin{cases} 1, & f_2 < s < 1, \\ \dfrac{s-f_1}{f_2-f_1}, & f_1 < s < f_2, \\ 0, & 0 < s < f_1. \end{cases} \tag{4}$$

Whenever all frontal sub-segments have a penetration depth less or equal to the current sub-segment, then snow is loaded. In the other case, when any frontal sub-segment has a penetration depth (ε_{max}) larger than the actual sub-segment, then snow is unloaded.

The shear force was modeled according to orthogonal metal cutting theory (Shaw [20]). For metal cutting as well as for ice (Lieu and Mote [10]) it is known that shearing is independent of the shearing velocity. We denote the ultimate shear pressure of snow by p^* (Mössner et al. [13,17]). When the lateral velocity v_l is positive, i.e. directed outward, the reaction force for a sub-segment is given by the shear strength of the snow

(5) $$F_s = p^* \varepsilon L, \qquad \text{for} \quad v_l > 0.$$

Finally, snow friction F_f, drag F_d and weight F_w were modeled by

(6) $$F_f = \mu(v)\, F_p, \quad \mu(v) = \mu_0 + \mu_1 v, \qquad F_d = \frac{1}{2}\rho\, C_d A\, v^2, \qquad F_w = mg.$$

Simulation of Turns

For the simulation of turns one has to solve the problem of keeping the balance of the skier. The resultant force F_R acting on the skier is the sum of weight and centrifugal force. The lateral component is given by

(7) $$F_L = \frac{mv^2}{r} - mg \sin\alpha \cos\beta\,,$$

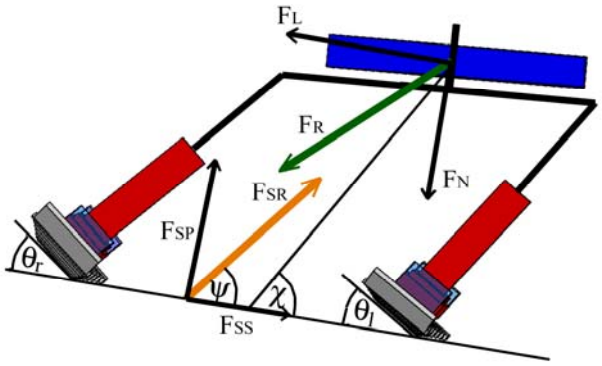

Fig. 2: View of the skier-ski system in the coronal plane, i.e. the given plane is normal to the snow surface and normal to the direction of movement. F_{SR} denotes the total snow reaction force, F_{SP} and F_{SS} the total snow penetration and shear force normal and parallel to the snow surface. F_R is the resultant force acting on the skier, F_L the lateral and F_N normal component with respect to the snow surface. θ_r and θ_l are the edge angles of right and left ski, χ inward lean angle of the skier, and ψ angle of the total snow reaction force F_{SR}.

where α denotes the inclination of the slope and β the traverse angle, i.e. the angle between the skier's velocity vector and the horizontal line of the slope. In the simulations a turn starts at 45° and finishes at 135°. In the first half of the turn centrifugal force and weight act in opposite directions and in the second half both are directed downwards. The resultant force leads to a reaction force of the snow denoted by F_{SR}. Its lateral component is given by

(8) $$F_{SS} = \sum_{left/right\ ski} F_s \,.$$

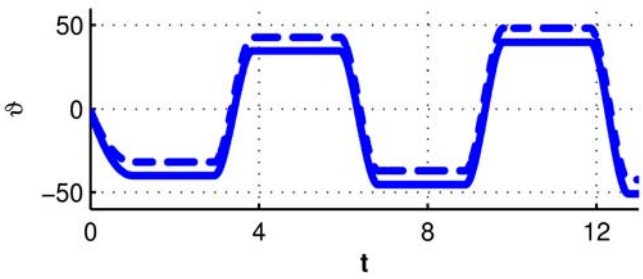

Fig. 3: Driving constraints for the edge angles of the XT ski. Solid line edge angle of the right ski θ_r [°] and dashed line edge angle of the left ski θ_l [°]. t [s] is the runtime in the simulation.

F_{SS} is limited by the shear strength of the snow. If F_L exceeds F_{SS} an accelerated side movement is initiated. This leads to skidding and for a large excess even to an overturn. To keep the balance, the skier has to choose his inward lean angle χ (see Fig. 2) approximately equal to the angle of the snow reaction force ψ. This can be achieved by carving without angulation. Then, the inward lean angle χ is equal to the complement $\chi=\theta^*+\pi/2$ of the mean edge angle $\theta^*=(\theta_r+\theta_l)/2$. Obeying these principles a *reference simulation* was established. In the first turn the skier skied with an edge angle of 40 and 32° for the outer and inner ski, respectively (Fig. 3). Because of the higher speed of the skier the edge angles had to be increased in each consecutive turn by 10%. The skier's center of mass was fixed in such a way that both skis were reasonably loaded and in longitudinal direction the center of mass was shifted 5 cm from the mounting point towards the tip of the skis.

Input Data

A carving ski (XT) with a projected ski length L_s of 1.65 m and a ski radius r_s of 12.5 m was implemented. The ski width w was taken from construction data. Bending stiffness EI and torsional stiffness GJ were determined in bending and torsion experiments. Finally, the spring constants used in the implementation were set to $C_B = EI/l$ and $C_T = GJ/l$ with l the length of a ski segment.

The simulations took place on a planar slope with an inclination α of 15°. Snow hardness H was set to 0.01 N/mm^3, the ultimate shear pressure of snow p^* to 0.025, 0.030, and 0.036 MPa for small, medium and large shearing strength of snow, respectively, and the snow friction coefficient was set to $\mu(v) = 0.080+0.004\ v$ with v the speed of the skier. This refers to quite soft snow. In the simulations the ski edge penetrated 5-10 mm into the snow. The mass of the skier including equipment m was 73 kg and his drag area C_dA was set to 0.6 m^2.

Parameter Studies

For the parameter studies the measured bending and torsional stiffness were varied from the reference simulation by ±20% (Fig. 4). To investigate the influence of snow conditions and edging of the skis the calculations were repeated for increased and decreased shearing strength of snow (±20%), and for increased edge angles (+10%). A sequence of turns of the skier was simulated for the reference and the varied data. For comparing the simulations we calculated the projection of the center of mass of the 10th segment of the right ski normal to the snow surface. The time-position function of this point is called the trajectory of the skier. This point is near to the mounting point of the right ski. In the simulations a turn ranged from β = 45-135°. For the calculation of the mean turn radius r we considered the part of the turn with traverse angles β ranging from 60-120°. The *mean turn radius r* is defined as the radius of the circle fitting that part of the skier's trajectory in the least squares sense. The maximum deviation of the trajectory to the least squares circle was less than 13 cm. So in the main part of the turn the trajectory of the skier was quite close to an arc of a circle. The largest deviations occurred in skidded turns with the small shearing strength of snow.

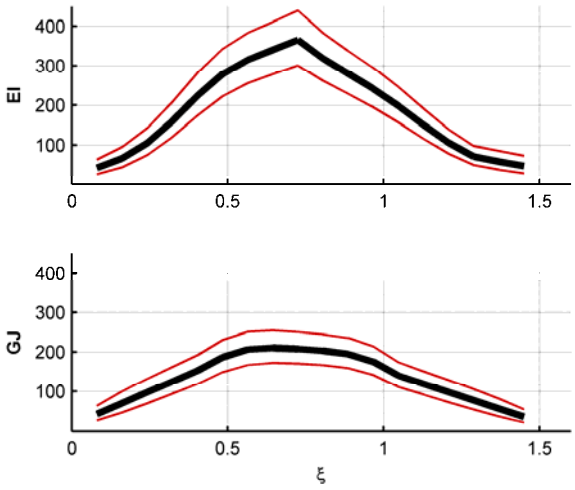

Fig. 4: Bending EI [Nm^2] and torsional GJ [Nm^2] stiffness used in the parameter studies. ξ [m] coordinate in longitudinal direction of the ski, 0 refers to the ski end and L_S to the titp of the ski. The thick line gives the value of the measurement on the real ski. Maximum variations are ±20% relative to the maximum of the stiffness data.

RESULTS

Simulation of Turns

For the implemented carving ski XT turns were computed by varying the snow conditions but using the measured ski stiffness. After a total runtime T of 13 s the skier finished 3-5 turns. His speed increased from 6 to 12 m/s. The skier went down the fall line of the slope approximately 110 m. In Fig. 5 the trajectories of the skier are given for the three values of the shearing strength of the snow. The markers in the

reference trajectory give the position for runtime differences of one second. The mean turn radius increased by 75% from 13.5-23.6 m, by 54% from 12.2-18.8 m, and by 34% from 11.7-15.8 m for small, medium, and large shearing strengths of the snow, respectively (Table 1). For purely carved turns on a rigid plane the turn radius should be equal to $r = r_S \cos\theta$ (Howe [7] or Lind and Sanders [11]) and hence decrease from 10.1-9.0 m. At this hypothetical turn radius the lateral snow reaction forces cannot compensate the centrifugal force. But with the actual turn radius, given in Table 1, the radial forces were almost in equilibrium in the main part of the turn, i.e. for *β* from 60-120°. But at the end of the turns, because of the gravitational force, the difference grew up to 100-200 N. This force excess caused a radial acceleration of 1-3 m/s^2 and an additional side movement of up to 1 m. A close look at the trajectories of the skier showed that the trajectory was circular in the main part of the turn, but not for the whole turn ranging from 45-135°. Especially at the end of the turns the skis considerably skidded. As a consequence the turn radius was noticeably increased. During the turns the skis were bent and twisted. For the medium shearing strength of snow the radius of the bending line (*bending radius*) decreased from 25.6-18.8 m and 43.6-33.6 m for the loaded and unloaded ski, respectively. The torsion twist was very small and varied from 0.8-2.1°. The corresponding radii of the bent ski edge were 9.8-8.9 m and 11.0-10.5 m. The increased ski bending was caused by the speed up of the skier and consequently a higher centrifugal force. The observed radii for the bent ski edge correspond to those predicted by Howe. The actual turn radii are considerably larger because of skidding.

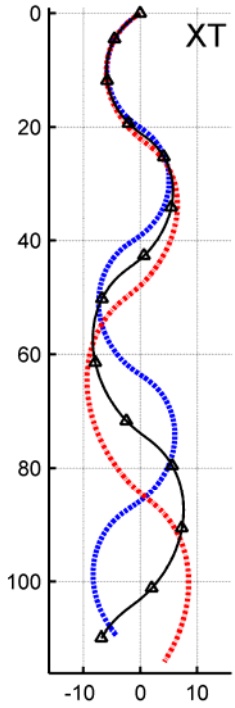

Fig. 5: Trajectory of the skier for small (dark grey), medium (black), and large (light grey) shearing strength of the snow.

Effect of Ski Stiffness

In Table 1 the mean turn radii are collected for increased/decreased bending and torsional stiffness, three values of the shearing strength of the snow, and two edge angles. A larger stiffness caused smaller turn radii when compared to the situation

with the same snow conditions and edge angles. Larger stiffness reduced skidding. The effect increased for higher speed of the skier, i.e. from turn 1 to 3, and for decreased shearing strength of the snow. In the 3rd turn a 20% larger stiffness caused 8, 5, and 1% smaller turn radii for small, medium and large shearing strength of snow. A 20% smaller stiffness caused an opposite effect of the same magnitude.

Edge Angle		normal			10 % enlarged		
Shear Strength of Snow		small	medium	high	small	medim	high
High Ski Stiffness	1st	13.0	12.1	11.7	12.3	11.7	11.3
	2nd	15.6	13.2	11.8	14.4	12.2	11.3
	3rd	21.7	17.7	15.6	19.7	16.1	14.5
Ski Siffness of Measurement	1st	13.5	12.2	11.7	12.7	11.7	11.3
	2nd	16.7	13.8	12.0	15.4	12.8	11.4
	3rd	23.6	18.8	15.7	21.5	17.2	14.2
Small Ski Stiffness	1st	13.9	12.4	11.7	13.1	11.8	11.3
	2nd	18.2	14.5	12.4	16.5	13.4	11.6
	3rd	25.6	19.8	16.0	23.2	18.1	14.6

Table 1: Mean turn radius r [m] for the first three turns in the simulation. Collected are the radii for two choices of the edge angle θ (Fig 3), for three types of snow (H = 0.010 N/mm^3 and p^* = 0.025, 0.030, and 0.036 MPa), and for 3 values of ski stiffness (Fig. 4).

Because of the increased stiffness the bending radius was increased by 1-5 m and the torsion angle decreased by 0.2-0.5°. The largest deviations occurred for soft snow or the 1st turn. The larger stiffness caused a larger bending radius of the ski and consequently a larger radius for the deflected ski edge. The mean penetration depth of both skis was increased by 4-5% from soft to stiff skis. Since the shearing force depends linearly on the penetration depth (Eq 5) the side force increased by 4-5%, too. Neither maximum penetration depth nor penetration depth of a single ski correlated with stiffness variation.

In the simulations with the enlarged edge angles we got similar results. Because of the larger edge angles the skis penetrated deeper into the snow and so shearing was reduced. Therefore, all effects due to varied stiffness were smaller. The effect that larger edge angles reduce skidding is used in praxis: Skilled skiers enlarge edge angles. We further did simulations for varied bending stiffness and torsional stiffness of the measurement. In this case the turn radii shifted 0.1-0.2 m towards the turn radii for the simulations with the measured stiffness. Because of the small overall torsion angle the effect of keeping the bending stiffness of the measurement and varying torsional stiffness was very small.

Discussion

A sequence of ski turns could be simulated. With the prescribed function for the edge angle (Fig. 3) weight and centrifugal force were in quite good balance with the snow reaction forces. The positioning of the center of mass corresponded to skiing without angulation. For small speed (1st turn) or large ultimate shear pressure of snow the lateral forces were of the same magnitude as the shearing strength of snow and so carved turns occurred. On the other hand for large speed (3rd turn) or small ultimate shear pressure of snow the shearing strength of snow was considerably exceeded. Depending on the excess the turns got highly skidded. At the start of a turn small side forces are necessary, since the centrifugal force and the lateral component of the gravitational force have opposite directions. At the end of a turn both point in downhill direction. Therefore skidding mainly occurs at the end of the turn. An increased edge angle causes a geometrical reduction of the turn radius, due to the $\cos\theta$ factor in Howe's formula. Additionally, shearing is reduced due to the larger penetration depth of the ski edge. With the shearing strengths of the snow used in the simulations it was not possible to carve without any skidding. Nevertheless, for the large shearing strength the skier carved quite well. So, in the simulation of the skier's trajectory the amount of skidding is a critical factor. Since the shear strength of snow linearly depends on the penetration depth of the skis, it is essential to use a suitable model to predict the penetration depth of the skis into the snow accurately. In a carved turn, the rear parts of the skis move in the track which the front parts dig into the snow. Compacted snow is not elastic - deformations remain. Such effects are considered by a hypoplastic constitutive equation. Therefore, for the snow a hypoplastic force-penetration relation was used obtaining a reasonable estimate of the penetration depth of the ski along its whole edge.

In the parameter study the effect of ski stiffness on the turn radius was investigated. Except in one case (large shearing strength of snow, enlarged edge angles, 3rd turn) a larger stiffness caused smaller turn radii. As expected, bending and torsional deformations decrease with increased stiffness. Less bending causes a larger radius for the deflected ski edge. According to Howe's theory this also should lead to a larger turn radius, but the opposite effect was observed. The problem arises, since Howe just looks at the geometry of the deflected ski edge to predict the turn radius. But, because of skidding, the ski does not follow the circle of the deflected ski edge. To get the actual turn radius one has to look at the resultant

force, applied by the skier, and the lateral snow reaction forces, which determine skidding. For small speed or high shearing strength of the snow these forces are in balance and consequently a carved turn occurs. In these cases ski stiffness has little effect on the turn radius (Table 1). On the other hand when speed gets large or when shearing strength of the snow gets small then skidding occurs. The ski skids as much as is necessary to obtain equilibrium between centrifugal force and lateral snow reaction forces. In this case the produced lateral force depends on the penetration depth of the ski into the snow. In our case we got an increased mean penetration depth for larger stiffness, consequently larger side forces and smaller turn radii. Different behavior may occur when the ski is embedded differently in the snow (e.g. Heinrich et al. [5] or Mössner et al. [16]). The small effect of the torsional stiffness should not be underestimated. In our case the torsion twist was, because of the flat terrain, 1-2° only. On a rough snow surface or in hilly terrain the torsion twist and therefore torsional stiffness will certainly cause effects.

Recently the model was improved by replacing the sledge with a Hanavan type skier (Heinrich et al. [6]). With this model it will be possible to get deeper insight in mechanical consequences of ski stiffness. We will get more realistic movements of the skier-ski system on the slope and the loading of the skis. Interesting questions are: How do skier movements interact with ski properties like stiffness and/or terrain properties.

ACKNOWLEDGMENTS

The investigation was supported by HTM Tyrolia.

REFERENCES

[1] Bruck, F, Lugner, P, and Schretter, H (2003) A Dynamic Model for the Performance of Carving, *14th ISSS, ASTM STP 1440*, RJ Johnson et al, Eds, ASTM, West Conshohocken, US-PA, pp 10–23.

[2] Casolo, F and Lorenzi, V (2001) Relevance of Ski Mechanical and Geometrical Properties in Carving Technique: A Dynamic Simulation, *Science and Skiing II*, E Müller et al, Eds, Verlag Dr Kovac, Hamburg, DE, pp 165–179.

[3] Federolf, PA (2005) Finite Element Simulation of a Carving Snow Ski, PhD thesis, ETH Zurich, CH.

[4] Fellin, W (2000) Hypoplastizität für Einsteiger (Hypoelasticity for Beginners), *Bautechnik*, Vol 77, pp 10–14. URL: *http://geotechnik.uibk.ac.at/res/hypopl.html*.

[5] Heinrich, D, Mössner, M, Kaps, P, Schretter, H, and Nachbauer, W (2006) Influence of Ski Bending Stiffness on the Turning Radius of Alpine Skis at Different Edging Angles and Velocities, *Eng of Sport 6*, EF Moritz et al, Eds, ISEA, Munich, DE, pp 207–212.

[6] Heinrich, D, Kaps, P, Mössner, M, Schretter, H and Nachbauer, W (2008) Computation of the Pressure Distribution Between Ski and Snow, this proceeding.

[7] Howe, J (2001) The New Skiing Mechanics. Including the Technology of Short Radius Carved Turn Skiing and the Claw Ski, *McIntire Publishing*, Waterford, US-ME.

[8] Kaps, P, Mössner, M, Nachbauer, W, and Stenberg, R (2001) Pressure Distribution Under a Ski During Carved Turns, *Science and Skiing II*, E Müller et al, Eds, *Verlag Dr Kovac*, Hamburg, DE, pp 180–202.

[9] Lieu, DK and Mote, CD (1985) Mechanics of the Turning Snow Ski, *5th ISSS, ASTM STP 860*, RJ Johnson et al, Eds, ASTM, Philadelphia, US-PA, pp 117–140.

[10] Lieu, DK and Mote, CD (1984) Experiments in the Machining of Ice at Negative Rake Angles, *J Glaciology*, Vol 30, pp 77–81.

[11] Lind, D and Sanders, SP (1996) The Physics of Skiing, Springer, New York, US-NY.

[12] LMS Virtual.Lab, LMS Int, Leuven, BE. E-mail: *info@lms.be*, URL: *http://www.lmsintl.com*

[13] Mössner, M (2006) Investigations on the Ski-Snow Contact in Alpine Skiing, Doctoral Thesis, Univ Innsbruck, AT. URL: *http://sport1.uibk.ac.at/mm/publ*

[14] Mössner, M, Heinrich, D, Schindelwig, K, Kaps, P, Lugner, P, Schmiedmayer, HB, Schretter, H and Nachbauer, W (2006) Modeling of the Ski-Snow Contact for a Carved Turn. *Eng of Sport 6*, EF Moritz et al, Eds, ISEA, Munich, DE, pp 195-200.

[15] Mössner, M, Heinrich, D, Kaps, P, Schretter, H and Nachbauer, W (2007) Computer Simulation of Consecutive Ski Turns. *17th ISSS*, ASTM, submitted.

[16] Mössner, M, Heinrich, D, Schretter, H, and Nachbauer, W (2006), Einfluss der Biege- und Torsionssteifigkeit von Skiern auf das Schwungverhalten (Effect of Bending and Torsional Stiffness of Skis on the Turn Radius), *11th Symp, Austrian Sport Science Assoc*, I Werner, et al, Eds, Innsbruck/Hungerburg, AT.

[17] Mössner, M, Nachbauer, W, Innerhofer, G, and Schretter, H (2003) Mechanical Properties of Snow on Ski Slopes, Poster presented at the 15th ISSS, St Moritz/Pontresina, CH. URL: *http://sport1.uibk.ac.at/mm/publ*

[18] Nordt, AA, Springer, GS, and Kollár, LP (1999) Simulation of a Turn on Alpine Skis, *Sports Eng*, Vol 2, pp 181–199.

[19] Renshaw, AA and Mote, CD (1991) A Model for the Turning Snow Ski*, 8th ISSS, ASTM STP 1104*, CD Mote et al, Eds, ASTM, Philadelphia, US-PA, pp 217–238.

[20] Shaw, MC (1984) Metal Cutting Principles, Oxford University Press, Oxford, GB.

[21] Tada, N and Hirano, Y (1999) Simulation of a Turning Ski Using Ice Cutting Data, *Sports Eng*, Vol 2, pp 55–64.